研究論文抄録

機械工学科

T. Ogawa : "An Efficient Numerical Algorithm for the Tree-Data Based Flow Solver", Computational Fluid Dynamics, 2000, Springer, pp.337-342, 2001.12
邦文題目：ツリー型データに基づく効率的な流体解析アルゴリズム

An efficient numerical algorithm is developed for the tree data structure which have been widely used for the adaptive Cartesian mesh method. A simple neighbor cell finding with a ¥lq¥lq{¥it pedigree}" and implementation of the implicit scheme and the Multigrid method are presented. It is found that the numerical schemes developed for the conventional flow solver can be easily implemented to the tree-data based flow solver.

橋本竹夫・波多野滋子：「こもり感の評価」音響技術, Vol.31, No.2, pp.42-44, 2002.6

自動車室内のように狭い閉空間の中では，ある速度で走行中にエンジンの爆発次数音など低周波数音の周波数が室内空間の共鳴周波数に一致して定在波が生じた場合，乗員の耳位置付近にその音圧の腹の部分が生じると鼓膜が圧迫される感覚が強まり不快なものとなり対策を要求される。これが，こもり感である。この感覚を定量化するためにこもり感に対する重み付け関数を主観評価より求め，音の大きさに対する影響も考慮した心理音響尺度であるBooming Indexを提案したところ，主観評価結果との良い対応が得られた。

T. Hashimoto and S. Hatano : "Effect of Seat Vibration to the Perception of Sound Quality under Long-Term Exposure of Car Interior Noise And Seat Vibration", Proceedings of the Inter-noise 2002, Session on Noise and Vibration Effect, 02-279, pp.1-8, 2002.8 (Invited paper)

The evaluation of sound quality of car interior noise is affected not only by car interior noise itself but also by seat vibration as well. In order to examine these effects quantitatively, subjective evaluation of car interior noise under long-term exposure of car interior noise together with seat vibration was conducted. As a result, significant variation of the perceived sound quality with time was found although the sound pressure level of the noise was remained the same. The effect of seat vibration to the perception of sound quality was also significant.

T. Hashimoto : "Temporal Variation of Sound Quality under Long-Term Exposure of Car Interior Noise and Seat-Floor Vibration", Fourum Acoustica, 2002, pp.1-6, 2002.9 (Iinvited paper)

Temporal variation of sound quality is observed under long-term exposure of car interior noise even in a case where the level of the sound remained constant. The effect is stronger for in the first one third of the total exposure time, i.e., one hour. The evaluation of sound quality is also affected by the simultaneous exposure of seat-floor vibrations. In order to examine these effects quantitatively, subjective evaluation of sound quality by the continuous SD method utilizing a personal computer as an input device has been conducted under long-term exposure of car interior noise and seat-floor vibrations.

広田明彦・笠原和夫：「切削抵抗と切りくず生成状態に及ぼすチップブレーカの影響」精密工学会誌, Vol.68, No.1, pp.130-135, 2002.1

In order to measure independently forces acting on rake face and on chip breaker, a tool dynamometer has been designed and constructed. Using step-type and groove-type chip breakers, orthogonal cutting and oblique cutting experiments have been performed. For a step-type

chip breaker, decreasing the distance between cutting edge and a chip breaker (chip breaker distance) gives the chip formation for tools with smaller tool-chip contact length than that of a conventional tool. The thrust force acting on the rake face decreases about 75% of that of the conventional tool. For groove-type chip breakers using tools with shortly restricted tool-chip contact lengths, it is found that the magnitudes of forces acting on the rake face are constant in spite of the chip breaker distance. This shows that the forces acting on the cutting point are scarcely influenced by external forces acting near the chip breaker. Even in the case of small broken chip produced at small chip breaker distance in oblique cutting, chip flow direction calculated from forces on the rake face approximately supports Stabler's chip flow rule.

弓削康平・江島　晋・阿部淳一:「耐衝突部材のトポロジー最適設計」第5回最適化シンポジウム講演論文集, No.02-03, pp.253-258, 2002.10

ここ数年，衝突時における乗員の安全性が自動車の性能を表す指標として評価されるようになり，車体構造の衝撃吸収性能の向上が求められている.特に，安全性という観点からすれば，衝撃吸収性能は車の商品価値と密接な関係があることから自動車メーカーを中心に研究が行われている。衝突問題の最適化では応答曲面法による寸法最適化の研究が先行している.これは最適化に伴う繰り返し計算数が他の方法に比べ相対的に少なくて済むためであり，衝突解析が多大な計算コストを要する点を考えると現実的な選択である。しかし，形状やトポロジーの最適化の場合は，設計変数の数が極めて多いために適当な応答曲面を効率よく確定するのは困難であり別な手法の開発が必要である。著者らはこれまで均質化法を用いたトポロジー最適化手法の応用研究の一環として塑性変形受ける構造物の最適設計手法を実施した。この手法は，許容設計領域内に一定量の物質を最適配置する手法であるが，その過程において異方性の強い様々な多孔質性複合材の弾塑性解析を均質化法によって解析することを必要としており，現在の計算機環境を持ってしても多大な計算コストを要することが問題となる。そこで，本研究では設計変数として局所的な密度を採用する密度法によって衝突エネルギーを吸収する最適設計を行うことを検討する。密度法は材料定数が密度のべき乗に比例する関数として表される仮想的な等方性材料を考え，許容設計領域内の局所的な密度分布を目的関数が最小となるよう決定する手法である。密度法は材料が等方性を有していると仮定するために，異方性の多孔質材を最適配置する均質化法に比べて計算時間が非常に短い。特に弾塑性問題では，等方性の塑性流れ則を用いることが可能あることより，塑性域の取り扱いが容易である。その反面，得られた最適形状にチェッカーボードやグレースケールといった曖昧なトポロジーが現れ，設計上しばしば問題となる場合がある。ここでは3次元動的弾塑性問題に本手法を適用し，図に示すような具体的な数値例より本手法の妥当性を検証する。さらに密度法で問題となるチェッカーボードやグレースケールの問題を解決するために重力制御関数を制約条件として導入し，設計・製造性まで考慮した構造最適化手法を提案する。最適化アルゴリズムには収束性が高く，複数制約を取り扱うことが可能なCONLIN法を適用した。なお，本最適化アルゴリズムでは最適解を導く過程で動的弾塑性解析を繰り返し実行することから，分散メモリー型並列計算を適用することにより計算コストの低減をはかる。

電気電子工学科

川又正太・青木正喜:「車載スリットカメラと路面マークを用いた位置・速度検出」画像電子学会誌, 31巻, 6号, 2002

簡単な路面マークを車載スリットカメラで撮影することにより，自車両の位置・速度を検出する手法を提案する。スリットカメラを路面向きに設置し，車両進行方向とスリットを垂直にして道路面を疑似二次元画像として撮影する。スリット画像上の路面マークの位置から，車線内の車両位置を検出する。路面マークに情報を付加することで詳細位置情報の取得が可能である。車両方向は画面上のマークの傾きから，車両速度は画面上のマークの長さから検出する。位置検出のための路面マークは四つの長方形で構成された中抜きのクロスマークを用いる。このクロスマークの交点を最小二乗法による直線近似を用いて検出することで，サブピクセル精度の位置測

定が可能である。テストコースでの実験と精度評価実験により提案した手法の有効性を実証した。

S. Katahara and M. Aoki : "Motion Estimation of Driver's Head from Nostrils Detection", Proceedings of the 5th Asian Conference on Computer Vision, pp.290-295, 2002. 1

We propose a method of estimating driver's head movement by tracking a pair of nostrils. Nostrils clearly appear as a pair of dark areas in a facial image. Shape of nostrils have little influence of deformation compared to eyes. We use a concentric circular mask or density difference mask to detect difference of image density. We represent nostril position by a center of gravity of extracted nostril region, and apply moving average to a sequence of the detected nostrils positions. We decide reference positions of nostrils through a procedure that an interval of moving average is fixed into a standard cycle of model driver's head motion. We estimate driver's head movement from a difference between detected nostrils position and reference nostrils position. Cycle of driver's head movement is available for a measure of monitoring driving condition. Experimental results show the effectiveness of our proposed method.

S. Katahara, T. Izumi, S. Kawamata and M. Aoki : "Traffic Flow Measurement Using Double Slit Image", 9th World Congress on Intelligent Transport Systems, 3071, TP029, 2002.10

We propose a video based one directional traffic flow measurement method using line sensor camera. Line sensor camera is inherently provided with the high resolution and flexible line capturing speed. Line sensor camera outputs pseudo two-dimensional image that consists of space domain and time domain. We detect occupancy, time headway and time between two cars from information along time axis in a slit image. We extract vehicles using fundamental image processing. In double slit configuration, we detect spot speed of vehicles by the time difference of its appearance at each slit. We also restore normalized vehicle images (recovered line sensor output images in the case that a capturing speed of a camera would be synchronized with a vehicle speed). Using line sensor camera in double slit configuration, we estimate vehicle length, space headway and distance between two cars. We count traffic volume, rate of flow, occupancy, time mean speed, average time headway and average time between two cars, as macroscopic traffic flow parameters for designated measurement interval. We represent top-view of normalized vehicle images. The normalized images are available for classification and identification of vehicles.

T. Ishigohka, M. Kobayashi, A. Ninomiya, S. Nomura, R. Shimada and Y. Sato : "Fabrication and Test of Force-Balanced-Coil Type Air-Core Superconducting Transformer Using Parallel Conductor", IEEE Trans. on Applied Superconductivity, Vol.12, No.1, pp.816-819, 2002.3

邦文題目：並列平行導体を用いた力平衡コイル型空心超電導変圧器の試作と試験

Superconducting winding can provide very large ampere-turns. So, an air-core type superconducting transformers can be designed. An air-core superconducting transformer has following merits;

(i) light weight,
(ii) elimination of iron loss;
(iii) reduction of insulation burden to ground potential;
(iv) mitigation of inrush current;
(v) reduction of noise caused by magnetostriction.

However, in case of an air-core transformer, the absence of iron-core means reduction of structural member. In case of an actual large-scale transformer, the electromagnetic force would be one of the most important factors that determine the basic design of device, size, cost, etc..

In order to reduce the electromagnetic force we introduced the configuration of the "Force-balanced-Coil" for the air-core transformer.

We fabricated an experimental transformer using superconducting windings with a parallel conductor configuration. Its fundamental tests were carried out.

Through the experiment, we confirmed the fun-

damental characteristics of the transformer. The obtained maximum output was about 1 kVA for the primary/secondary voltages of 20/10 V, respectively.

H. Mizutori, A. Ninomiya and T. Ishigohka : "Magnetic Circuit Switching Element with Superconducting Coil", IEEE Trans. on Applied Superconductivity, Vol.12, No.1, pp.859-862, 2002.3
邦文題目：超電導コイルを用いた磁気回路スイッチング要素

In an existing power system, high-current circuit breakers are widely used. Meanwhile, we propose a new switching device using a switching of magnetic paths. It is a magnetic circuit switch activated by On/Off of superconducting coils wound on iron core-legs. We have carried out an experiment using a small experimental device with two superconducting coils (control coils). When the control coil is shorted, the voltage of the output coil in the shorted side becomes 0 V because the magnetic flux is blocked completely by the induced shielding current of the superconducting coil. It was confirmed that the current of the superconducting coil is decided by the turn-ratio of the coils both experimentally and theoretically. Therefore, it was assured that any tremendous over-current does not flow in the shorted superconducting control coils. After this, we applied this device into a model of two-circuit transmission system and confirmed the fundamental behavior in case of a line fault. The experimental result shows that the fault current is suppressed almost perfectly and the transmission system can continue the power transmission without any intermission.

Y. Nomoto, A. Ninomiya and T. Ishigohka : "Fabrication and Test of a Superconducting Generator with Ring Windings", IEEE Trans. on Applied Superconductivity, Vol.12, No.1, pp.863-867, 2002.3
邦文題目：環状巻線を有する超電導発電機の試作と試験

Application of superconductivity to electric machines can bring about wider alternatives to the fundamental configuration comparing with the conventional counterparts. As well known, multi-phase AC electric machines can be easily realized with ring-winding configuration. Because a multi-phase machine is effective to obtain smooth DC voltage with low ripples, it would be attractive as a generator for the exclusive use in HVDC power transmission system. Besides, the ring-winding configuration is suitable for high-voltage design. Armature windings do not cross each other as in the conventional windings. In order to confirm the fundamental characteristics, a multi-phase generator with superconducting ring windings was manufactured and examined. The armature is composed of nine coils, i.e., the number of phases is nine. It has also a superconducting field winding. The machine does not have iron core except for the outer magnetic shield made of laminated iron. Well-balanced nine phase output voltages with phase angle differences of 40 degree were obtained. When full-wave rectification circuits were connected to each armature winding directly, a smooth DC voltage and a current with sufficiently low ripple factor were obtained without any smoothing circuits and transformer banks.

T. Hemmi, A. Ninomiya, T. Ishigohka, et al. : "Transient Behavior of Bi2223/Ag HTS Tape for Sharp Rising Current", IEEE Trans. on Applied Superconductivity, Vol.12, No.1, pp.1422-1425, 2002.3
邦文題目：急峻増加電流に対するBi2223/Ag高温超電導テープ線材の過渡特性

For the application of HTS composite conductor to electric power apparatuses such as power cables or transformers, its stability under a short circuit fault condition is very important. In an actual power system, we have to take into consideration the large short circuit current. Meanwhile, so far, the only available HTS conductor for a practical application seems to be Bi2223/Ag HTS tape. So, we have started a study on a transient behavior of Bi2223/Ag HTS tapes during a short circuit condition in liquid nitrogen under self-magnetic field.

In this paper, we have carried out an experiment and a numerical study on a transient of the voltage and the thermal behavior of HTS tape. In the experiment, the current was increased rapidly from a

small steady state level to a large level higher than the critical current. We have produced the calculation code that simulates the transient phenomena. The experimental results were compared with the numerical ones.

K. Arai, A. Ninomiya, T. Ishigohka, K. Takano, K. Matsui, P. C. Michael, R. F. Vieira, N. N. Martovetsky, K. Kaiho, H. Nakajima, Y. Takahashi, T. Kato, T. Ando, H. Tsuji and K. Okuno : "Acoustic Emission during DC Operations of the ITER Central Solenoid Model Coil", IEEE Transactions on Applied Superconductivity, Vol.12, No.1, pp.504-507, 2002.3

邦文題目：ITER中心ソレノイド・モデルコイルの直流通電時のAE

Acoustic emission (AE) signals from the Central Solenoid (CS) model coil developed in ITER program were studied during direct current (DC) operation. Estimation of the AE energy from the coil indicates close correlation between the AE energy and AC losses in the cable-in-conduit (CIC) conductor. This correlation comes from motions of the cables and de-bonding of strands in the cable-in-conduit (CIC) conductors during repeated charging of the coil. The AE measurements clearly indicated the existence of mechanical disturbances even in the case cases where the voltage spikes observed in the balance voltages were comparable to the noise level. In the case of the CS model coil, the locations of the mechanical disturbances could be determined using AE signals in combination with information from voltage spikes correlated with the AE signals.

石郷岡猛・二ノ宮晃・藤浪達也・上條弘貴・藤本浩之：「減衰振動パルス磁界によるバルク超電導体の消磁」日本AEM学会誌, Vol.10, No.2, pp.143-147, 2002.6

近年，磁気浮上式鉄道，磁気分離，NMR等の分野への高温超電導体の強力な永久磁石としての応用の研究がなされつつある。これらの応用のためには，一旦着磁したバルク高温超電導体を消磁する技術が実用的見地から見て重要になる。通常，臨界温度以上まで昇温して常電導状態に転移させて消磁することは勿論可能であるが，高温超電導体に熱サイクルを経験させなければならず，ひび割れや特性劣化などの原因になる可能性がある。一方，超電導マグネットによる強磁界を用いて準静的に消磁する事も可能であるが，超電導マグネットがある場所でしか消磁させることが出来ない。このため，コンデンサバンクに充電した電荷を常電導の銅コイルに放電させて得られる減衰振動パルス磁界による消磁，および，小型の交流発電機を用いた減衰振動パルス磁界による消磁を行った

石郷岡猛・二ノ宮晃・押田圭太・水取寛満・上條弘貴・藤本浩之：「減衰振動パルス磁界によるバルク超電導体の消磁実験」日本AEM学会誌, Vol.10, No.3, pp.335-338, 2002.9

バルク高温超電導体は，浮上式鉄道，磁気分離，等々への応用で強力な永久磁石として期待されている。この応用のためには，実用的見地から見て，一旦着磁したバルク高温超電導体を，消磁することが必要になる。この場合，臨界温度以上まで昇温して常電導状態に転移させて消磁できるが，高温超電導体に熱サイクルを経験させることになり，特性劣化が起こる可能性がある。また，超電導マグネットによる強磁界を用いて準静的に消磁できるが，超電導マグネットが必要になる。著者等は，コンデンサバンクと常電導銅コイルとを用い，それによる減衰振動パルス磁界を用いて消磁する実験を行った。

二ノ宮晃・新井和昭・高野克敏・石郷岡猛・海保勝之・中嶋秀夫・杉本　誠・奥野　清・辻　博史・N. MARTOVETSKY・I. Rodin・CSモデル・コイル実験グループ：「ITER TFインサート・コイルのAE特性」低温工学, Vol.37, No.10, pp.35-43, 2002

The Central Solenoid Model Coil (CS model coil) program was established in 1992 as one of the projects for the Engineering Design Activities (EDA) of the International Thermonuclear Experimental Reactor (ITER). In the year 2001, we carried out several kinds of tests using a CS model coil and a Toroidal Field(TF) insert coil. In the experiments, we measured the acoustic emission (AE) signals emitted from these coils. This was the first attempt to measure AE from the insert coil directly, as AE sensors were not attached during the previous tests conducted in 2000. In this paper, we focus our discussion on the AE signals emitted from the TF insert coil. Two kinds of data acquisition methods for the AE signals were utilized during the series of excitations: full waveform recording and AE envelope

recording. Observation of the AE signals showed that the disturbances in the TF insert coil decreased with the iteration number of excitation as judged from the instantaneous AE energies and AE event count. Furthermore, we confirmed that the AE had constant distributions during a 1,000-time-cyclic test under a back-ground-field of 13 T using the CS model coil. Therefore, we obtained an important experimental result in that the TF insert coil was highly stable throughout the series of experiments

N. Martovetsky, P. Michael, J. Minervini, A. Radovinsky, M. Takayasu, C.Y. Gung, R. Thome, T. Ando, T. Isono, K. Hamada T. Kato, K. Kawano, N. Koizumi, K. Matsui, H. Nakajima, G. Nishijima, Y. Nunoya, M. Sugimoto, Y. Takahashi, H. Tsuji, D. Bessette, K. Okuno, N. Mitchell, M. Ricci, R. Zanino, L. Svoldi, K, Arai and A. Ninomiya : "Test of the ITER Central Solenoid Model Coil and CS Insert", IEEE Transactions on Applied Superconductivity, Vol.12, No.1, pp.600-605, 2002.3

邦文題目：ITER中心ソレノイド・モデルコイルとCSインサートの試験

The Central Solenoid Model Coil(CSMC) was designed and built from 1993 to 1999 by ITER collaboration between the U.S. and Japan, with contributions from the European Union and Russia Federation. The main goal of the project was to establish the superconducting magnet technology necessary for a large-scale fusion experimental reactor. Three heavily instrumented insert coils were built to cover a wide operational space for testing. The CS Insert, built by Japan, was tested in April-August of 2000. The TF Insert, built by Russian Federation, will be tested in the fall of 2001. The NbAl Insert, built by Japan, will be tested in 2002. The testing takes place in the CSMC Test Facility at the Japan Atomic Energy Research Institute, Naka, Japan. The CSMC was charged successfully without training to its design current of 46 kA to produce 13T in the magnet bore. The stored energy at 46 kA was 640 MJ. This paper presents the main results of the CSMC and the CS Insert testing- magnet critical parameters, ac losses, joint performance, quench characteristics and some results of the post-test analysis.

犬塚俊康・瓜生芳久・小柳文子：「電源が系統内の潮流と負荷に及ぼす貢献度の検討」電気学会論文誌，電力エネルギー部門誌，122巻，17号，p.791，2002.7

電力産業の規制緩和の世界的流れを受けて，多くの国で電力需給体制の見直しが進んでいる。送配電分野においては国の情勢によって様々な形態が見られるものの，発電部門に関してはおおよその国で競争原理の導入が進んでいる。中でも，独立発電事業者（IPP：Independent Power Producer）が入札により参入する事が可能になり，競争原理の導入によって，電気料金の低減が促されると予測される。

このような状況下で，電力システム全体が効率的に運用され，電力市場での効率的な競争が維持されるためには，送電ネットワークの適切な利用ルールやコスト等を反映した公平な電気料金下での運営が不可欠である。これらの問題の解決法の一つとして「貢献度」の概念がある。すなわち，送電システム内での電力の詳細情報，特に「各電源から各負荷にどれだけ電力を供給しているか」「各電源がどれくらい送電線を利用しているか」の評価を行うために，各電源の「貢献度」の概念を導入し，評価を行うことで，より簡易に各電源の負荷と送電線潮流に与える影響を評価することができる。

この論文では，実際にこの概念を利用できるよう，「貢献度」を簡易に計算できるアルゴリズムの構築を目指している。具体的には，この「貢献度」を用いて，複雑かつループ状の電力系統を「電源の領域」ごとにグループ分けして放射状の簡単な形状で表現し算出する手法，及び任意の系統状態に対し柔軟に領域分け・貢献度の算出を行うアルゴリズムを示している。本手法を実規模系統である電気学会EAST10機系統モデルにおいて2種類の系統状態に対し適用し，検討を行った。

Y. Saito and K. Tokuda : "Suppressed Boron-Penetration Through Surface-Nitrided Ultrathin Oxide Films Prepared by Fluorination and Subsequent Exposure to Atomic Nitrogen", Jpn. J. Applied Physics, Part 1, Vol.41, No.3A, pp.1515-1518, 2002.3

邦文題目：フッ化および原子状窒素処理により表面窒化した極薄シリコン酸化膜におけるホウ素貫通抑制効果

Several percent of nitrogen was incorporated only near the top surfaces of thermally grown oxides, by surface fluorination at room temperature

followed by an atomic nitrogen treatment at 550℃. The dependences of the nitrogen content and the thickness of the nitrided layer on the process condition were studied by angle-resolved X-ray photoelectron spectroscopy. A model of the nitridation process was also proposed. MOS capacitors with boron-doped polycrystalline silicon gates were fabricated using the nitrided ultrathin oxide. From the capacitance-voltage measurements we confirmed that the nitrided oxide would more effectively prevent boron penetration in comparison with the conventional oxide films. The proposed technique is a unique process for obtaining high-quality ultrathin dielectrics.

Y. Saito : "Characteristics of Plasmaless Dry Etching of Silicon-Related Materials Using Chlorine Trifluoride Gas", Sensors and Materials, Vol.14, No.5, pp.231-237, 2002.7

邦文題目：三フッ化塩素を用いたシリコン系材料のプラズマレスドライエッチングの特性

Silicon substrates and thermally grown oxide films were exposed to ClF_3 gas at various temperatures between room temperature and 600℃. Above room temperature, the activation energy of the silicon etch rate is 0.18 eV. The activation energy of SiO_2 etch rate below 400℃ is estimated to be 0.12+/-0.01 eV. The obtained etch selectivity of silicon with respect to the SiO_2 is 100-300 between room temperature and 400℃. An enhanced etch rate is observed for the n-type silicon with low resistivity near room temperature. The ClF_3 gas, which has appropriate vapor pressure, has useful properties not only for in-situ cleaning but also for micro-machining of silicon-related materials.

鈴木誠一・丸田武史・中村吉希：「カイワレ種子の成長に対する溶液環境中の金属イオンの影響と側抑制」電気学会部門誌, C分冊, Vol.122-C, pp.1686-1691, 2002

The effects of metal ion concentration in the culture medium of Rahpanus sativus were investigated. A seed of R.sativus is known to uptake metal ion for its root growth, which produces ion influx and electrical potential along the root. However, in the very early stage of root growth, a R.sativus seed releases large amount of metal ion to the ambient medium. The reason and mechanism of this early ion release was still in question. We have examined the root growth of single or double seed culture, and shown that the single seed can not grow in small volume culture medium because of the high ion concentration. On the other hand, in case of two seeds, this happened only to one seed and another one grows almost normally. This growth regulation by ion concentration can be explained as a lateral inhibition mechanism of seeds sprayed in a small area.

鈴木誠 一・望月道博・肥後昭男：「シリケイトゲルを用いたマイクロバイオリアクタの試作」電気学会C部門, 医用・生体工学研究会報告(大分), MBE-02-27, pp.17-20, 2002

A micro reactor using hydro gel as enzyme immobilization medium was fabricated by photolithography technique and reaction efficiency was measured in connection with the flow rate of substrate solution. The enzymatic function of protein is one of the most important aspects in the analysis and applicat ion of biological phenomena. However, the complex functionality of a cell is realized by organizing each function of protein molecule, in terms of compartmentation, diffusion, affinity, active and passive transport and so on. Diffusion control by the porous material was investigated in this paper as a model system of enzyme reaction in a cell. The results suggest that the diffusion in sub-micro meter scale is not a major restriction of reaction rate but the osmotic pressure plays an important roll.

鈴木誠一・中村　聡：「音源定位における頭部回転運動の影響の検討」電気学会C部門, 医用・生体工学研究会, MBE-02-66, pp.33-38, 2002

We have investigated the resolution of human auditory localization in connection with the stereo sound with ambient echo for the assistance of visually impaired person. The localization of computer synthesized stereo sound was difficult for stationary state. To improve the resolution of the localization, we employed the moving sound tracking the head motion. The resolution was improved by the factor of 2, partly because of the comparison of sound spectra for different direction,

and partly because of the higher accuracy of head motion compared with the localization.

S. Suzuki,Y. Kanakogi, I. Tachibana, T. Hagiwara and M. Iida : "Development of an Optical Sensor for Multi-Component Immuno-Detection", Proc. IEEE Sensors 2002(Orlando), 2002.5

An optical immunosensor free from the background noise of nonspecific adsorption was developed. Fluorescent labeled antibody molecule was immobilized on quartz substrate. The molecular motion of the antibody was measured by the fluorescence anisotropy with evanescent excitation apparatus. It was demonstrated that the antigen binding to the antibody was detected as anisotropy change, without interference of nonspecific molecule. The high performance in discriminating specific molecule suggest the possibility of multi component detection for the instant diagnosis of infection and protein screening. Integration of this kind of sensor is expected for the application in determination or infectious disease or proteome analysis.

四倉達夫・K. Binsted・F. Nielsen・C. Pinhanez・鉄谷信二・中津良平・森島繁生：「HyperMask：３次元顔モデルを用いた仮面の構築」電子情報通信学会論文誌ＤⅡ, Vol.J85-D-Ⅱ, No.1, pp.36-45, 2002.1

HyperMaskとは従来単一の顔表情や人物を表現する仮面の概念を進化させ，1つの仮面からあゆる表情や人物を自由に生成および表現可能なシステムである。本システムを用いることで，その仮面を装着した役者の表現の幅や新しい演出方法が生み出されていくと考えられる。顔の表出手法として，仮面に装着された5つのLEDを，カメラにより追跡することで仮面の位置および方向を求め，プロジェクタによって算出されたパラメータをもとに顔画像の投影を行う。また投影されている顔画像は演技者の音声を分析することによりリアルタイムで音声同期して口形状のアニメーションを行い，顔表情や人物の切り替えはユーザが任意に選択可能である。本論文ではHyperMaskシステムを用いた演出支援装置を紹介し，新たな仮面の表現技法の確立を目指す。

T. Yotsukura, S. Morishima, F. Nielsen, K. Binsted, C. Pinhanez："HyperMask：Projecting a Talking Head onto a Real Object", The Visual Computer, International Journal of Computer Graphics, Springer, Vol.18, No.2, pp.111-120, 2002.3

HyperMask is a system which projects an animated face onto a physical mask worn by an actor. As the mask moves within a prescribed area, its position and orientation are detected by a camera and the projected image changes with respect to the viewpoint of the audience. The lips of the projected face are automatically synthesized in real time with the voice of the actor, who also controls the facial expressions. As a theatrical tool, HyperMask enables a new style of storytelling. As a prototype system, we put a self-contained HyperMask system in a trolley (disguised as a linen cart), so that it projects onto the mask worn by the actor pushing the trolley.

四倉達夫・森島繁生・他：「カスタマイズ性を考慮した擬人化音声対話ソフトウェアツールキットの設計」情報処理学会論文誌, 43巻, 7号, pp.2249-2263, 2002.6

本論文では，擬人化音声対話エージェントを将来のヒューマンインタフェースの重要な技術要素として位置づけ，研究開発の共通プラットフォームとなりうる高いカスタマイズ可能性を備えたソフトウェアツールキットの実現を目指し，それに必要な要素とその実現技術について論じる。今後のヒューマンインタフェース技術において，コンピュータがあたかも一個の人間として振る舞い，人間の顔や姿を持ち，ユーザと音声言語で対話するようにすることは，大きな目標の１つである。このような研究開発を進めるにあたっては，多分野の協力が必要であり，研究成果を集積していくための共通プラットフォームが必要である。それには，音声認識，音声合成，画像合成，対話制御などの基本モジュールと，それらを統合制御する仕組みが必要である。さらに，個性の表現や広い応用などのためには，各モジュールは高い基本機能のみならずカスタマイズ可能性が重要である。このため，筆者らは，顔画像が用意に交換可能で，音声合成が話者適応可能で，対話制御の記述変更が容易で，さらにこれらの機能モジュール自体を別のモジュールに差し替えることが容易であるなどの特徴を持つ擬人化音声対話エージェントシステムを構想し，実装した。いくつかの簡単な対話タスクについてエージェントを試作し，必要な機能に関する達成度を確認した。

森島繁生:「HAIにおけるエージェントのリアリティとコミュニケーションギャップ」人工知能学会誌, Vol.17, No.6, pp.687-692, 2002.11

マルチモーダルを駆使して人間と機械がフェーストゥーフェースで対話する環境を実現しようとする試みは,ポストGUIに向けて特に注目を集める分野となっている。エージェントのリアリティに関する議論もしばしば行われるが,カートゥーンキャラクターのような本来の動きというものがもともと存在せず架空に仕立て上げられたものに多くの人々が愛着を覚えるのに比して,人間そのもののクローンを実現する技術は実物が存在するがゆえに要求される条件も自ずと厳しくなり,僅かな粗も無視することはできない。したがって,現時点ではHAIの人物描写において生身の人間と同等のリアリティを追及し,まさにビリーバブルなエージェントを実現するには,まだまだ年月を要するであろうし,音声認識・合成・対話技術とのバランスも考慮しなくてはならない。本稿で述べるHAIのための人物描写は,あらかじめオリジナルのオンラインもしくはオフラインの映像が存在することを前提としている。イメージベースレンダリングやビデオリライトとも関連するが,完全にイメージのみに拘るのではなく,幾何構造も考慮したハイブリッド構造をとり,より柔軟性を持たせている。さらにHuman-Agent-Human, すなわち人間と人間との対話の中間にエージェントが介在して,そのコミュニケーションギャップを埋めることに重点を置き,対話生成自体は人間が行うものとしてそこには関知しない。ここでいうコミュニケーションギャップとは,言語の障壁やノンバーバル情報の欠如に起因するもので,このギャップを認識・合成技術を駆使して埋め合わせし,より円滑なコミュニケーションを実現することが,エージェントの果たす役割と位置づけする。認識技術により,オリジナルの映像中からターゲットとすべき情報のみを抽出し,合成技術によってこの情報を置き換える。以下第2章では,表情モデリングの現状について述べる。また3章ではオリジナルの映像シーンから顔情報を抽出する方法について述べ,4章ではコミュニケーションギャップの一例として言語障壁をとりあげ,音声翻訳とのリップシンクの実現について述べる。5章では別の応用としてのインタラクティブムービーシステムを紹介する。6章はこのリップシンクの評価方法を紹介し,7章では,より高いリアリティ実現に向けて,表情の動的なモデリング手法としての顔面筋肉モデルと,頭髪のダイナミクスモデルについて述べる。8章では現在進行中の音声対話擬人化エージェントプロジェクトについて紹介する。

応用化学科

佐藤功治・大友良則・川崎兼司・尾崎義治:「金属アルコキシドからの酸化物還元法によるInSb膜の合成」Journal of the Ceramic Society of Japan, 110[3], pp.173-179, 2002.3

A new synthetic route based on a solution chemistry was developed for a compound semiconductor indium antimonide(InSb). Considering the moisture sensitive properties of metal alkoxides, indium antimonide was synthesized by reduction of $InSbO_4$, which was prepared by hydrolysis of the corresponding metal alkoxides as starting materials. InSb-alkoxide solution was prepared by two ways: one is mixed method in which In-alkoxide solution and Sb-alkoxide solution were mixed simply, and the other is continuous method using the reaction of indium chloride with Na-alkoxide in the presence of Sb-alkoxide in ethanol. Hydrolysis products by both methods were crystallized to $InSbO_4$ by heat-treatment at 780℃ in air. InSb was obtained by heat-treatment of hydrolysis product prepared by the continuous method at 400℃ in H_2, but it wasn't obtained from hydrolysis product prepared by the mixed method. The primary particle size of hydrolysis products was about 8 nm in diameters. The wet hydrolysis product was well mixed with ethylcellulose and terpineol by a three-roll mill to form printing paste. The paste was screen-printed on slide glass substrates, transformed to InSb film by heat-treatment at 400℃ in H_2.

川崎兼司・尾崎義治:「金属アルコキシドからのジルコニアバルーンの合成」Journal of the Ceramic Society of Japan, 110[8], pp.748-754, 2002.8

Zirconia balloons were synthesized from zirconium tert-n-butoxide in F/B/F(formamide / benzene/formamide) emulsion. Zirconium tert-n-

butoxide in benzene ranging from 0.5 to 2.0mol·l^{-1} was dispersed in formamide. The formed droplets of zirconium tert-n-butoxide in benzene could be solidified in formamide because solvent benzene was extracted by formamide; these solidified droplets were hydrolyzed with water in order to obtain zirconia precursor balloons. Zirconia precursor balloons were successfully obtained from a 1.2mol·l^{-1} solution of zirconium tert-n-butoxide in benzene. Diameter of zirconia precursor balloons was 150 to 450 μm. Zirconia precursor balloons could be heat-treated at 1300℃ to form zirconia balloons without damage of the balloon structure. The diameter of zirconia balloons was in the renge between 100 and 400 μm. Weight loss and shrinkage observed during heat-treatment were 34.5mass% and 45vol%, respectively Zirconia balloons consisted of grains with 0.2 μm in diameter. Pores with 50nm in diameter existed on their surface and wall cross-section.

A. Katoh, Y. Hikita, M. Harata, J. Ohkanda, T. Tsubomura, A. Higuchi, R. Saito and K. Harada : "3-Hydroxy-4(1*H*)-Pyridinone-Containing Linear and Cyclic Hexapeptides and Their Iron(III) Complexes : Synthesis, Property, and the Growth-Promotion Activity", *Heterocycles*, Vol.55, No.11, pp.2171-2187, 2001.12

邦文題目：3-ヒドロキシ-4(1*H*)-ピリジノン含有鎖状及び環状ヘキサペプチドとそれらの鉄(III)錯体：合成，性質及び生長促進活性

Linear and cyclic hexapeptides composed of ε-(3-hydroxy-1,4-dihydro-2-methyl-4-oxo-1-pyridyl)-L-norleucine and glycine or β-alanine residue have been successfully synthesized. These hexapeptides formed 1:1 iron(III) complexes at neutral pH region. Glycine linear (8a)- and β-alanine cyclic hexapeptide (10)-iron(III) complexes predominantly existed in Δ-configuration, while β-alanine linear hexapeptide (8b)-iron(III) complex existed in Λ-one. The relative stability constants of 8a, 8b, and 10-iron(III) complexes were estimated to be 31.6, 33.4, and 31.7, respectively. From iron(III) removal from human transferin, linear hexapeptides (8a, b) were found to efficiently remove iron(III) compared with desferrioxamine B. The growth-promotion activity was also discussed.

A. Katoh, T. Tsukahara, R. Saito, K. K. Ghosh, Y. Yoshikawa, Y. Kojima, A. Tamura and H. Sakurai : "An Extremely High Insulin-Mimetic Activity of Bis(1,4-dihydro-2-methyl-1-phenyl-4-thioxo-3-pyridinolato)zinc(II) Complex", *Chemistry Letters*, No.1, pp.114-115, 2002

邦文題目：ビス(1,4-ジヒドロ-2-メチル-1-フェニル-4-チオキソ-3-ピリジノラト)亜鉛(II)錯体の顕著な高インスリン様活性

Vanadyl and zinc(II) complexes with $VO(O_2S_2)$ and $Zn(O_2S_2)$ coordination mode, respectively, were synthesized. Among them, bis(1,4-dihydro-2-methyl-1-phenyl-4-thioxo-3-pyridinolato)zinc (II) complex exhibited an extremely high insulin-mimetic activity (IC_{50} = 0.04 mM when IC_{50} value of a positive control, $VOSO_4$ was estimated to be 1.0 mM) compared to vanadyl and zinc(II) complexes reported previously.

加藤明良・野添紀希・後藤直樹・高野浩司・齋藤良太：「代表的なペプチド結合形成法を用いた際の副反応に関する研究」成蹊大学工学研究報告, 39巻, 2号, pp.7-13, 2002.9

The coupling of 8-iodooctanoic acid and *p*-toluidine by means of the WSC·HCl-HOBt method afforded not the corresponding *N*-(8-iodooctanoyl)-4-methylalanine but two types of products, *N*-(8-chlorooctanoyl)-4-methylalanine (4a) and *N*-[8-(benzotriazol-1'-yl)oxyoctanoyl]-4-methyl-alanine (4b) in 42 and 24% yields, respectively. The coupling of the same reagents in the presence of Et_3N·HCl by means of DCC-HOBt method also gave a mixture of compounds (4a) and (4b) in 21 and 29% yields, respectively, suggesting that ammonium hydrochloride efficiently acted as a Cl^- source on the replacement of I by Cl. On the basis of these model reactions, the coupling of *N*-nicotinoyl-L-(*p*-amino)phenylalanine methyl ester and 8-iodooctanoic or 11-iodoundecanoic acid was carried out by the DCC-HOBt method to give the desired products, *N*-nicotinoyl-L-*p*-(8-iodooctanoyl) aminophenylalanine methyl ester (3a) and *N*-nicotinoyl-L-*p*-(11-iodoundecanoyl)-aminophenylalanine methyl ester (3b) in 41 and

50% yields, respectively.

R. Saito, M. Kaneda, T. Wada, A. Katoh and Y. Inoue : "First Asymmetric Photosensitization in Supercritical Fluid : Exceptionally High Pressure/Density Dependence of Optical Yield in Photosensitized Enantiodifferentiating Isomerization of Cyclooctene", *Chemistry Letters*, No.8, pp.860-861, 2002

邦文題目：超臨界流体中における不斉光増感反応：シクロオクテンの光増感エナンチオ区別異性化反応における光学収率の顕著な圧力/密度依存性

The photosensitized enantiodifferentiating isomerization of (*Z*)-cyclooctene (**1Z**) in supercritical carbon dioxide has been performed for the first time. The critical control of the enantiomeric excess (ee) of chiral product, (*E*)-cyclooctene (1E), and even the switching of the product's chirality were achieved through a small change of pressure particularly in the low-density region near the critical density. Quantitative evaluation of these ee changes was achieved by estimating differential activation volumes between the diastereomeric transition states of the reaction.

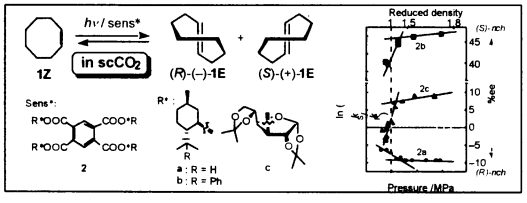

R. Saito, K. K. Ghosh, K. Harada and A. Katoh : "Microbial Growth-Promotion Activity of 3-Hydroxymonoazine- and *N*-Hydroxydiazine-Type Heterocycles", *Yakugaku Zasshi*, Vol.122, No.9, pp.703-705, 2002

邦文題目：3-ヒドロキシモノアジン及び*N*-ヒドロキシジアジン系複素環化合物の微生物生長促進活性能

Three 3-hydroxymonoazine- and three *N*-hydroxydiazine-type heterocycles were tested whether they act as artificial siderophores toward *Aureobacterium flavescens* JG-9 (ATCC No. 25091). Among them, 1-hydroxy-3,5,6-trimethyl-2(1*H*)-pyrazinone (**3**) showed the highest growth-promotion activity comparable to desferrioxamine B (DFB), a natural trihydroxamate siderophore, at 48.5 mM or above, followed by 1-hydroxy-5,6-dimethyl-2(1*H*)-pyrazinone (**2**), 1-hydroxy-4,6-dimethyl-2(1*H*)-pyrimidinone (**1**), and 3-hydroxy-2-methyl-1-phenyl- 4 (1*H*)-pyridinone (**6**), while 3-hydroxy-1,2-dimethyl-4(1*H*)-pyridinone (**5**) did not show the bioactivity. These results are the first examples of *N*-hydroxydiazine-type heterocycles acting as artificial siderophores for *A. flavescens* JG-9.

K. Kurita, M. Inoue and M. Harata : "Graft Copolymerization of Methyl Methacrylate onto Mercaptochitin and Some Properties of the Resulting Hybrid Materials", Biomacromolecules, 3, pp.147-152, 2002

邦文題目：メルカプトキチンへのメチルメタクリレートのグラフト共重合と生成する複合材料の特性

The graft copolymerization of methyl methacrylate onto mercaptochitin and some properties of the resulting graft copolymers have been studied. Methyl methacrylate was efficiently graft copolymerized onto mercaptochitin in dimethyl sulfoxide, and the grafting percentage reached 1300% under appropriate conditions. Although the side-chain ester groups were resistant to aqueous alkali, hydrolysis could be achieved with a mixture of aqueous sodium hydroxide and dimethyl sulfoxide. Subsequent treatment with acetic anhydride in methanol transformed the sodium carboxylate groups into carboxyl groups. Although the graft copolymers exhibited an improved affinity for organic solvents, those having sodium carboxylate or carboxyl units were characterized by a much more enhanced solubility and were soluble in common solvents. The hygroscopic nature of chitin decreased with an increase in the grafting extent but increased significantly upon hydrolysis of the ester groups. The enzymatic degradability of the graft copolymers, as evaluated with lysozyme, was also dependent on the grafting extent and much higher than that of the original chitin. DSC measurements revealed the presence of a glass transition phenomenon, which could be ascribed to the poly(methyl methacrylate) side chain.

濱野裕之・田原聖隆・小島紀徳・山田興一：「乾燥地における飽和透水係数の原位置測定および土層構造解析」農業土木学会論文集，69 (6), pp.739-746 (216, 33-40),

2001.12

圃場飽和透水係数測定には現在多くの方法が提案されているが，乾燥地における測定報告は少なく，また土壌構造を考慮した測定法の検討はなされてこなかった。そこで本研究では半乾燥地である西オーストラリア州，レオノラ地域を対象に，変水位法，ゲルフパーミアメーター法，シリンダーインテークレート試験を用いた測定を行い，各測定方法の特徴を明らかにするとともに，土壌構造解析を行った。その結果，裸地土壌における変水位法の変動係数は30.6-58.9%と小さく，垂直方向の測定値の平均値はゲルフパーミアメーター法の結果とほぼ一致した。3つの原理，測定部位の異なる飽和透水係数測定の適用により，飽和透水係数の複合的判断および土層構造解析が可能であることを示した。

濱野裕之・田原聖隆・小島紀徳・山田興一：「乾燥地における飽和透水係数の原位置測定および数値計算による測定精度評価」農業土木学会論文集，70(2)，pp.145-153 (218, 19-27), 2002.4

原位置飽和透水係数測定方法の比較・検討は農地については多数行われてきたが，乾燥地における測定結果報告は少なく，そのうえ各測定方法が有する測定誤差，解析誤差を考慮した測定方法の比較・検討はなされてこなかった。本研究では，西オーストラリア，レオノラ地域を対象として，数値計算を用いた測定条件や解析方法の定量的評価，ゲルフパーミアメーター法における不透水層の影響，シリンダーインテークレート試験によるクラストの透水性の評価を行った。その結果，ゲルフパーミアメーター法の測定において深さ46cmに存在する不透水層により，浸入流量は約10%減少することが明らかになった。土壌表層に形成されているクラスト層の透水係数は，下層土の値より3桁も小さい値をとることが明らかになった。また土壌構造が有する様々な不均一性から生ずる偏差や誤差の定量的解析が，数値計算と複数の測定による結果の比較により可能であることを示した。

小島紀徳・石田丈介・濱野裕之・田原聖隆：「保水材混合による土壌の透水性・保水性の変化」農業土木学会論文集，70 (3), pp.313-319 (219, 19-25), 2002.6

乾燥地での植林にあたっては土壌中の水移動を制御し，蒸発，流失量を極力削減し，その分を樹木からの蒸散に変えることが必要である。そのために保水材を土壌に混合して透水性，保水性を改善することが提案されている。本研究では豊浦砂に高分子保水材（SAP），ボーキサイト，ピートをそれぞれ一定割合で混合し定量的に透水性，保水性の挙動変化を把握した。また，各保水材の最適な利用法についても考察した。その結果，どの保水材を混合しても，混合率の増加に伴い透水性は減少し，保水性は増加する傾向が定量的に明らかになった。ピートを混合すると4.2＞pF＞1.8で大きな保水性の向上が確認された。焼成ボーキサイトでは，pF＞4.2での体積含水率が大幅に増加し，特に乾燥地において有効である可能性が示唆された。

H. Liu, C. Chen and T. Kojima："Theoretical Simulation of Entrained Flow IGCC Gasifiers：Effect of Mixture Fraction Fluctuation on Reaction Owing to Turbulent Flow", Energy & Fuels, 2002, 16, pp.1280-1286, 2002.9

邦文題目：気流層ガス化炉の理論的シミュレーション：乱流による混合分率の変動が反応に与える影響

A three dimensional numerical model was developed for a two stage entrained flow coal gasifier. In the model, the coal devolatilization, volatile and char combustion, char-H_2O and char-CO_2 gasification, and gas phase shift reaction were taken into account in accordance with the actual process. Four mixture fractions were used to simulate the coal gasification. The influence of turbulence on gas composition was taken into account by a pdf model with a clipped Gaussian distribution function. The model uses conventional numerical methods and sub-models to calculate gas and particle temperatures, gas and particle velocity, mean turbulent kinetic energy and turbulent energy of dissipation, gas species composition, particle trajectory, extent of reaction and radiant heat flux. The effect of mixture fraction fluctuation on the overall gasification characteristics owing to turbulent flow was investigated for gasification in an IGCC gasifier. It was revealed that the fluctuation of mixturefraction of gases produced from devolatilization and char-O_2 reactions has an important influence on not only distributions of temperature and gas composition, but also cold gas efficiency and heating value of product gas. On the other hand, the fluctuation of mixture fraction of gases produced from char-CO_2

and char-H_2O reactions has only a limited effect. The including of the fluctuation of mixture fraction smoothens the distribution of temperature. However, the fluctuation of mixture fraction concerning all the reactions has little effect on the distribution of particle concentration. For gasification in an entrained flow IGCC gasifier, with little influence on the validity of the simulated results, the neglecting of the fluctuation of mixture fraction of gases produced from char-CO_2 and char-H_2O reactions can significantly shorten the calculation time. On the other hand, the fluctuation of mixture fraction of gases produced from devolatilization and char-O_2 reaction can not be neglected. Comparison between prediction and measurement suggests that including fluctuation of mixture gives a better prediction.

T. Tsubomura, M. Ito and T. Fujita : "Conformation of 18-Membered Tetraimino Macrocyclic Complex : Structure of Two Metal Complexes and Molecular Mechanics Study", Bull. Chem. Soc. Jpn., Vol.75, No.11, pp.2393-2402, 2002.11.

邦文題目：18員環テトライミノ大環状錯体のコンホメーション：新規二錯体の構造と分子力場法による研究

The conformations of metal complexes of 18-membered tetraimino macrocycles have been studied. A correlation between the bond length of the metal-nitrogen bond and the conformation of the macrocycle has been found in the published X-ray data. Molecular mechanics (MM) calculations based on the Points-On-a-Sphere (POS) method reproduce the correlation. The effect of the MM force constants on the conformation of the ligand has been extensively studied. The MM study clarified that the conformation of the macrocycle is principally determined by the length of the coordination bond and that the methyl groups substituted at the imine carbon plays an important role in the conformation of the macrocycles. Two X-ray crystal structure analyses of macrocycle L^H complexes, $[Ba(L^H)(ClO_4)_2$ $Ba(L^H)$ $(H_2O)(ClO_4)(\mu\text{-}ClO_4)]$ and $[Sr(L^H)(ClO_4)_2]$ were included in the study to complement the structural data.

S. Hara, H. Hasuo, M. Nakasato, Y. Higaki and Y. Totani : "Modification of Soybean Phospholipids by Enzymatic Transacylation, Journal of Oleo Science, Vol.51, No.6, pp.417-421, 2002

邦文題目：酵素的アシル基変換反応による大豆リン脂質の改質

Modified glycerophospholipids with expected novel physiological functions were prepared by introducing different acyl groups into soybean phospholipids. The method was based on the enzymatic transesterification of phospholipids with monoacylglycerol (MG) or diacylglycerol (DG). The transacylation ratios reached 46-59% and nearly quantitative recovery of phospholipids was obtained in the case of transacylation of phospholipids with MGs having C12 to C18 saturated and monounsaturated acyl groups. With C18:2-MG or C18:3-MG, however, transacylation ratios were less than ca. 20%. MGs with C4 to C8 saturated acyl groups also gave very low transacylation ratios, but the ratios were moderately improved by using DGs with C6 and C8 acyl groups.

It is considered from a series of the results that higher transacylated phospholipids might be obtained by repeating transacylations owing to be able to recover the phospholipids quantitatively after the reaction because MG with longer acyl groups than C10 or DG with C8 acyl groups acted as acyl donors and replacement for essential water, to suppress the simultaneous hydrolysis, in an enzymatic reaction.

原　節子・戸谷洋一郎：「構造リン脂質の調製」オレオサイエンス, 2巻, 1号, pp.13-17, 2002

Structured phospholipids were prepared by the lipase-catalyzed transacylation of soy-phospholipids with monoacylglycerol (MG) of different fatty acids under the non-aqueous system. The various phospholipids comprised saturated fatty acids with carbon number of 4-18, and oleic, linoleic, linolenic, icosapentaenoic and docosahexaenoic acids could be obtained with high yields by transacylation used with MG of corresponding fatty acids. The repeating reaction process is available to raise the transacylation ratio, since the non–aqueous transacylation is not accompanied by the hydrolysis

the hydrolysis as a side reaction catalyzed by lipase.

A. Higuchi, K. Shirano, M. Harashima, B. O. Yoon, M. Hara, M. Hattori and K. Imamura : "Chemically Modified Polysulfone Hollow Fibers with Vinylpyrrolidone Having Improved Blood Compatibility", Biomaterials, 23(13), pp.2659-2666, 2002

邦文題目：生体適合性を有するヴィニルピロリドン表面修飾ポリサルフォン中空糸膜の調製

Hydrophilic polysulfone membranes (PVP-PSf) were prepared from polysulfone membranes covalently conjugated with polyvinylpyrrolidone (PVP) on the surface. The immobilized amount of vinylpyrrolidone on PVP-PSf membranes was controlled by the amount of vinylpyrrolidone monomer in the reaction solution and the reaction time. The PVP-PSf membranes were found to be the most hydrophilic membranes among the polysulfone and surface-modified polysulfone membranes prepared in this study. This is explained by the long hydrophilic side chain of polyvinylpyrrolidone on the PVP-PSf membranes which contributes to the hydrophilic wiper on the hydrophobic PSf membranes. It was found that PVP-PSf membranes gave lower protein adsorption from a plasma solution than polysulfone and other surface-modified membranes ($p < 0.01$). This is attributed to the hydrophilic surface of the PVP-PSf membranes, because the hydrophilic surface is known to reduce the protein adsorption on the membranes. The PVP-PSf membranes showed a much suppressed number of adhering platelets on the surface than polysulfone and other surface-modified membranes ($p < 0.01$). It is suggested that the hydrophilic surface of the PVP-PSf membranes without ionic groups causes the suppression of platelet adhesion on the PVP-PSf membranes and that the long hydrophilic side chain of polyvinylpyrrolidone on PVP-PSf membranes contributes to the hydrophilic and hemocompatible wipers on the surface of the hydrophobic PSf membranes

A. Higuchi, H. Yomogita, B. O. Yoon, T. Kojima, M. Hara, S. Maniwa and M. Saitoh : "Optical Resolution of Amino Acid by Ultrafiltration Using Recognition Sites of DNA", J. Membrane Sci., 205(1-2), pp.203-212, 2002

邦文題目：DNAの認識サイトを用いた限外ろ過法によるアミノ酸の光学分割

Ultrafiltration experiments for the optical resolution of racemic phenylalanine were investigated in a DNA solution system and by using immobilized DNA membranes. D-Phenylalanine preferentially existed in the totally collected permeate solution in the ultrafiltration of DNA and racemic phenylalanine solution (i.e. DNA solution system), although the separation factor ranged from more than unity or less than unity depending on the permeation time when the concentration of DNA was less than 0.5ppm. This is explained by the fact that DNA sometimes releases phenylalanine depending on the permeation time in the dilute DNA solution (i.e. 0.01–0.5ppm) due to the conformational change of DNA as a function of time. On the other hand, L-phenylalanine preferentially existed in the permeate solution and D-phenylalanine preferentially existed in the concentrate solution in the ultrafiltration of racemic phenylalanine through the immobilized DNA membranes. This indicates that L-phenylalanine preferentially enters into the pores of the immobilized DNA membranes and permeates through the membranes due to the interaction between DNA and L-phenylalanine. The immobilized DNA membranes were categorized as channel type membranes.

A. Higuchi, B. O. Yoon, T. Asano, K. Nakaegawa, S. Miki, M. Hara, Zhenjie He and Ingo Pinnau : "Separation of Endocrine Disruptors from Aqueous Solutions by Pervaporation", J. Membrane Sci., 198, pp.311-320, 2002

邦文題目：浸透気化法による水溶液からの内分泌かく乱物質の分離

Separation of endocrine disrupting chemicals from aqueous solutions was investigated by pervaporation using hydrophobic polydimethylsiloxane (PDMS) membranes. 1,2-Dibromo-3-chloropropane (DBCP, MW=236.4 g/mol), which is commonly used as a soil fumigant in the agricultural industry, was selected as a model endocrine

disrupting compound. DBCP could be separated very efficiently from very dilute aqueous solutions through PDMS membranes by pervaporation when the vacuum line between pervaporation cell and a cold trap on the permeate side was heated to 150 °C. The separation factor of endocrine disruptors over water depended significantly on membrane thickness. This effect was caused by concentration polarization of the highly permeable endocrine disruptor. As the thickness of the PDMS membranes decreased, concentration polarization caused a significant reduction in separation factor.

Pervaporation of other organic compounds from dilute aqueous solutions through PDMS membranes was also performed. The separation factors of the organic compounds could not be correlated well with their molecular size. As expected, hydrophobic organic chemicals showed higher separation factors than those of hydrophilic organic compounds using hydrophobic PDMS membranes.

M. Morita, S. Kajiyama, T. Kai, D. Rau and T. Sakurai : "Physicochemical Control of Valence in Pluminescence of Cr(III) And V(III, IV) Complexes Embedded in Xero-Gel and Sol-Gel SiO_2 Glasses", J. Lumin., 94-95, pp.91-95, 2001.12

Sol-gel silica glasses doped with transition metal complexes were prepared by the sol-gel-method using metal complexes such as (a) $Cr(III)(AA)_3$ (AA= acetylacetonato), (b) Cr(III) tris-nuclear basic acetate (Cr-trimer), (c) $V(III)(AA)_3$, and (d) $V(IV)O(AA)_2$. Luminescence, time-resolved luminescence, decay times, excitation and absorption spectra were measured at temperatures between 300 and 10 K to investigate the valences of metal ions in mesoporous matrices. Sharp lines at 13,000 cm^{-1} due to single Cr(III) ions and exchange-coupled Cr(III) pairs are found in glasses, annealed at temperatures below 150℃, doped with (a) and (b), respectively. In the glasses annealed above 500℃, a structured broad band is found to be due to the Ligand-to-Metal Charge Transfer (LMCT) transition by generation of either $[Cr(VI)O_4]^{2-}$ or $[V(V)O_4]^{3-}$ complex ions. The spectral shapes, lifetimes and vibronic structures in glasses (c) and (d) are understood easily by assuming the following thermo-chemical processes by increase of annealing temperatures : (d)$[V(III)(AA)_3]$ · c)$[V(IV)O(AA)_2]$ $[V(V)O_4]^{3-}$. Moreover, the coexistence of both Cr(III) and Cr(VI) ions is confirmed in some glasses (b) prepared under mild chemical conditions.

経営・情報工学科

竹越香苗・岩崎　学：「2段階抽出による2つの二項確率の検定におけるサンプルサイズの推定と検出力の評価」応用統計学, Vol.30, No.2, pp.91-106, 2001.12.

臨床研究などの計画では複数の段階に分けて標本を抽出することが多い。複数段階抽出の下でサンプルサイズを推定する場合，必要となるパラメータが未知であるため，ほとんどの場合2段階目以降のサンプルサイズは前の段階から得られた結果より推定されたパラメータを用いて定められる。このときサンプルサイズ推定に必要なパラメータが既知である場合の「真の検出力」と未知である場合の「推定された検出力」がどのように異なるかを知ることが重要である。本論文では2段階抽出において2つの二項確率間の検定に対するサンプルサイズの推定を行ない，「真の検出力」と「推定された検出力」を比較する。

岩崎　学：「非線型方程式の単純反復解法とその統計的応用」応用統計学, Vol.30, No.2, pp.107-118, 2001.12.

母集団分布の未知パラメータθに関する統計的推測では，方程式$f(\theta)=0$の解法を含むことが多い。本論では，$f(\theta)=0$を$\theta=g(\theta)$と変形して得られる反復解法$\theta^{(n+1)}=g(\theta^{(n)})$を議論する。まず，反復法の一意的な収束のためのこれまでとは若干異なる十分条件を与え，実際の解法の性質を吟味する。次に，興味ある統計的問題に対して本解法を適用した事例をいくつか紹介する。本解法は表計算ソフトで簡単に計算でき，実際の統計的データ解析に加え，統計教育の講義ならびに演習で有用である。

M. Iwasaki and N. Hidaka : "Notes on the Central and Shortest Confidence Intervals for a Binomial Parameter", Japanese Journal of Biometrics, Vol.22, No.1&2, pp.1-13, 2002. 2.
邦文題目：二項確率の最短および中心信頼区間に関する注意。

Several characteristics of confidence intervals for a binomial parameter are considered. In particular confidence intervals when zero success is observed are of our interest. There have been proposed two constructing methods intervals for such cases, which seems to be troublesome. In order to resolve the conflict we examine the methods from the viewpoint of coverage probabilities of the central and shortest confidence intervals. After a brief review of several constructing methods of confidence intervals, a simple iterative procedure to find the shortest interval is introduced. Then, in terms of actual coverage probabilities, we examine the properties of several intervals. Some guidelines in selecting appropriate interval are provided for dealing with practical problems.

上田　徹・住舎俊宏：「どの野球選手の攻撃力が優れているだろうか」オペレーションズ・リサーチ, Vol.47, No.3, pp.137-141, 2002.3

プロ野球選手の打撃成績をDEA（包絡分析）法により評価している。DEA 法の基本モデルでは評価対象にとって都合の悪い項目は無視して評価されるため予想外に高い評価値が出ることがある。そこで，本研究では，入力，出力項目の選定に注意しつつウェイトに付けるべき様々な制約（領域限定法）について検討している。また，パ・リーグとセ・リーグを異なる評価システムととらえ，2システムの違いを考慮した評価，年俸に対する仕事の度合いの評価，打順の評価も行っている。

T. Ueda and K. Hoshino : "Estimation of Firms Efficiencies Using Kalman Filter and Stochastic Efficiency Model", 16th Triennial Conference of the International Federation of Operational Research Societies, p.62, 2002.7

Firms are being operated over long years. Thus, we should evaluate their efficiencies, based on their historical data relating to finance. We shrink each historical data into a distribution function with a mean and a variance estimated by Kalman filter. Then, we apply stochastic efficiency model to shrunk data. We propose a new efficiency measure called by the modified efficiency score and compare it with existing measures.

M. Ohkura, H. Nara, Y. Nakagawa, M. Tauchi, T. Murakami and M. Kitano : "A Tactile Forewarning Sign for Informing Visually Impaired Independent Pedestrians of the Position and the Direction of a Tactile Guiding Line Serving as an Aid to Street Crossing", J. Science of Labour, Vol.77, No.12, pp.490-495, 2001.12
邦文題目：視覚障害者用道路横断帯（エスコートゾーン）の位置と方向を知らせる触覚的手がかりに関する基礎研究

Tactile guiding lines (TGLs) have been developed to assist visually impaired independent pedestrians in crossing intersections. These lines have been installed on crosswalk areas for practical use. Each TGL is 30 cm in width and consists of rows of dome-shaped dots (4.5 mm in height and 20 mm in diameter) made of acrylic resin. Each row is arranged to be perpendicular to the direction of crossing and consists of 12 pieces with dot-shape protrusions. The distance between the rows is 75 mm and that between the dots is 25 mm. When users step on the rows of dome-shaped dots, they perceive them as nearly raised lines because of the close distance between dots. The TGL is called as an "Escort Zone" in Japan. Our previous studies indicated that the TGL was a useful means of assisting visually impaired pedestrians, but reliable clues to the exact position and the direction of the TGL were needed at the entrance of the crosswalk to improve the usability of the TGL. In the previous field experiment, a crosswalk was selected where a tactile sign was placed on the sidewalk quite near the TGL. The sign consisted of a row of dome-shaped dots, similar to the TGL, arranged to be perpendicular to the direction of crossing. Blind subjects participated in the experiment stated that they could use it effectively to know the position and the di-

rection of the TGL. The tactile sign was thus considered to be one of the practical ideas of informing users the position and the direction of the TGL at the entrance of crosswalk. However, a question arose about whether users could get the reliable information about the position and the direction from only one row of dome-shaped dots. So an experiment was planned to investigate how many rows of dome-shaped dots were most suitable for users' performance.

Two test platforms, platforms A and B, were made on the roof of a building of our university. On both platforms, Braille tiles(dot and bar tiles; each 30x30 cm in size) were arranged to simulate an entrance of crosswalk. Three pieces of the dot tiles were arranged along the step of the imaginary curb. Four pieces of the bar tiles were arranged next to the set of the dot tiles, in the way that the bars projected a line of travel. In addition a tactile sign was placed next to the set of the dot tiles at the opposite side of the bar tiles only for platform B (as seen in fig.3). Three kinds of tactile signs were prepared; one, two and three rows of dome-shaped dots made of acrylic resin and similar to the TGL were formed on a 30x30 cm wooden board. Twenty-four blindfold sighted subjects were asked to start walking from the edge of the bar tiles far from the dot tiles and to stop on the dot tile under the condition of no tactile sign or on the tactile sign under the other three conditions for a short period for establishing their orientation, then to restart walking to straightly cross the imaginary crosswalk of 10 meters long. The subjects' walking path in crossing and their subjective evaluations of the tactile signs were recorded.

The tactile sign consisting of two rows brought the least deviation of the walking path from the expected straight line. This conditions was evaluated the most favourably by the subjects.

嶋田葉子・池上敦子・大倉元宏：「タスク分析に基づく看護婦勤務表作成支援システムのユーザインタフェースの開発と評価」人間工学，Vol.38, No.5, pp.261-271, 2002.10

現在，看護婦勤務表は，婦長や主任が手書きの表を利用して作成するのが一般的である。勤務表は，看護の質だけでなく看護婦の生活パターンや収入にも影響することから，作成者は毎回気を配りながら長時間かけて作成している。この負担を軽減するため，コンピュータによる看護婦勤務表作成支援システムが開発されてきているが，本研究では，ユーザーがコンピュータの操作に煩わされることなくスケジューリングに専念できるような支援システムの開発を目的とした。前の研究で行った手書きによる現状作業のタスク分析から，既存の支援システムにはなかった人間の思考作業に役立つユーザーインターフェース機能がいくつか明らかになっている。そこで今回は，この機能を備えた支援システムを開発し，現場のユーザーに評価してもらった。その結果，実際に実行できる勤務表を作成することができ，特にタスク分析結果を基に設計した機能に高い評価が得られた。

窪田　悟：「LCDの画素密度と表示文字の読取りやすさとの関係」映像情報メディア学会誌，56巻，8号，pp.1304-1308, 2002.8

We investigated the effects of pixel density, character matrix size, and character size on the subjective legibility of liquid-crystal displays (LCDs). At a 30-cm viewing distance, 50 subjects assessed the legibility under 33 different display conditions, we used 6×4.5 photographs to simulate the LCDs. We found that the character matrix for Japanese characters should be more than 10 x 10 pixels when the characters are smaller than 2.7 mm. For characters 2.7 to 3.5 mm, the character matrixes should be 15 x 15 to 17 x 17 for single-stroke characters, and 22 x 21 to 27 x 27 for double-stroke characters. These results show that the preferred character matrix depends on pixel density, character size, and stroke width. The preferred stroke width for Japanese characters is 200 to 300 μm. From the legibility point of view, the pixel density of displays should be increased to 250 or 300 pixels per inch.

芝田京子・川口忠雄・他：「ゴルフスイングのダイナミクスと運動制御（第1報）：ゴルフスイングを表現する評価モデルの構築」精密工学会誌, Vol.68, No.3, pp.473-490, 2002.3

The purpose of this study is to propose brand-new 2-dimentional model to estimate golfer's swing motion. This model was constructed to take singular value decomposition and prototype with approximative polygon to the typical points of a body picked up a series of 2-dimentional photographs. Usually, many results of analysis by using 3-dimentional method are reported. There is no discussion about relationship between the results of 2-dimentional method and 3-dimentional method. Further more, there is no information about superiority of 2-dimentional method. According to this study the following results were obtained. The relationship between actual golfer's swing motion and whole rhythm represented by the combined motions of each body joint has been solved with singular value decomposition. And 2-dimentional prototype cleared how to use each body joint. As a result, 2-dimentional method threw light on difficult problem to reproduce the golfer's swing motion.

芝田京子・村野次郎・川口忠雄：「腰痛防止姿勢制御装置付き車椅子の開発研究（第1報）：腰痛評価を考慮した人体等価モデルの構築」精密工学会誌, Vol.68, No.11, pp.1441-1446, 2002.11

Now, a wheelchair is being used widely. However many users have troubled for lumbago. In this research, lumbago prevention was approached by biomechanics and control engineering. As premise, lumbago was defined as rotation of a pelvis and change of a lumbar vertebra curve being the causes. Therefore, it approximates posture to the ideal vertebral column curvature, in order to prevent lumbago. Then, first, the inclined angle of a pelvis and the curve radius of a lumbar vertebra in various seating positions were considered. Based on it, in order to reproduce posture change on a computer and evaluate lumbago, human equivalent model was created in analyzing anatomy in detail. Here, modeling was carried out by three sides, frame, mass and muscular. Posture change was simulated using the model which simplified the previous one on the software DADS. The simulation result of the evaluation model was able to express mathematically change of a lumbar vertebra curve as evaluation of an ache. As a result, it was verified that the built model is appropriate to evaluate lumbago. Furthermore this paper proposed the wheelchair with posture control for lumbago prevention adopting a swing seat, a lumbar support, and a pelvis support.

Y. Kanda, H. Nagao and T. Naruo："Estimation of a Tennis Racket Power Using Three-Dimensional Finite Element Analysis", Engineering of Sport 4 / ed. by S. Ujihashi and S.J. Haake, Blackwell Publishing, pp.207-214, 2002.9

邦文題目：３次元有限要素解析によるテニスラケットの反発力評価

Tennis racket power is a primary factor of the performance and can be evaluated as the coefficient of restitution (COR) for the impact between a ball and a racket. The actual tension after stringing and the reduction of the frame rigidity due to the compressive axial force induced by the string tension are investigated. Since the COR depends on string tension, frame stiffness, and the gripping condition, the effects of these parameters on the COR were investigated precisely using finite element analysis. It was found that the COR value increases in general as the string tension decreases, or as the frame rigidity increases.

Y. Hayashi, Y. Fukuda and M. Kudo：“Investigation on Changes in Surface Composition of Float Glass：Mechanisms and Effects on the Mechanical Properties”, Surf. Science, pp.507-510, pp.872-876, 2002.9

邦文題目：フロートグラスの表面創世変化の解明：機械的特性に対するメカニズムと効果

Changes brought about in the mechanical properties on the top and bottom faces of float glass by weathering were compared, and factors

governing these properties were investigated. Resistance to the formation of cracks was shown to be improved by wethering, and the level of improvement was significantly higher for the top face compared with that for the bottom face. Secondary ion mass spectrometry depth profiles have shown that a hydrated layer, which originates from the ion exchenge reaction between sodium and hydrogen ions, forms more easily on the top face than on the bottom face during weathering. The significantly improved resistance to the formation of cracks on the top face can be explained by the low hardness of the hydrated layer. Furthermore, it has been proved that the Sn^{2+} ion suppresses the ion exchange reaction between sodium and hydrogen ions on the glass surface. Consequently, the thinner hydratedlayer on the bottom face can be ascribed to the existence of the polarisable Sn^{2+} ion, which penetrates into the bottom face of the float glass during the float process. These results lead to a method for the successful control of the ion exchenge reaction, which is important for controlling the mechanical properties of the float glass.

T. Kon : "Heavy Selectron Production with Exotic Signature in R-Parity Breaking Susy Models at E Gamma Colliders", Nucl. Instrum. Meth. A, Vol.472, pp.239-242, 2001.12

邦文題目：Rパリティ非保存模型における電子光子加速器での重いスカラー電子生成

We consider an R-parity breaking SUSY model in which a heavy scalar electron decays into a top quark. As the e-gamma colliders could be the most suitable machine for us to search for heavy selectrons, it is worth studing such an exotic signature of the selectron production at e-gamma colliders. We found that the selectron with mass about 300GeV could be searchable at the e-gamma colliders whose basic ee total energies are 500GeV.

N. Sasaki, S. Watanabe and M. Tsukada : "Visualization of Thermally Fluctuating Surface Structure in Noncontact AFM and Tip Effects on Fluctuation : Theoretical Study on Si(111)$\sqrt{3}\times\sqrt{3}$-Ag Surface", Physical Review Letters, Vol.88, pp.0461061-0461064, 2002.2

邦文題目：非接触AFMにおける熱揺らぎ表面構造の可視化と揺らぎに対する探針効果：Si(111)$\sqrt{3}\times\sqrt{3}$-Ag 表面に関する理論的研究

We investigated Noncontact Atomic-Force Microscopy images of a thermally fluctuating surface structures together with tip effects based on the first-principles electronic state calculation. As an example Si(111)$\sqrt{3}\times\sqrt{3}$-Ag ($\sqrt{3}$-Ag) surface is studied. We have succeeded in theoretically visualizing the thermal fluctuation of$\sqrt{3}$-Ag surface at room temperature, and reproducing the observed NC-AFM image for the first time. Pinnig effect of the thermal fluctuation of $¥sqrt{3}$-Ag surface by the tip is clarified. These results show a novel ability of Noncontact Atomic-Force Microscopy to modify the surface structure.

佐々木成朗・塚田　捷：「動的モード原子間力顕微鏡に現れる非保存的過程」表面科学，23巻，2号，pp.111-115, 2002.3

探針が誘起する非保存的な原子過程が動的モード原子間力顕微鏡のカンチレバーの動力学に与える効果を，時間平均を用いる摂動論をもとに理論的に解析した。非保存的過程の例として原子的な凝着を考える。凝着に由来するQ値の典型的な大きさのオーダーは10000と見積もられ，カンチレバー固有のQ値とほぼ同じ大きさになる。凝着による付加的な周波数シフトは10Hzのオーダーとなった。この周波数シフトは，探針の転回点がある閾値以下になると突然現れる。この特徴は半導体表面の化学的に活性の高いサイト上で，周波数シフトの不連続的なとびが実験的に観察される事の説明となる。

Y. Motoda, N. Sasaki and S. Watanabe : "Theoretical Study on Atomic and Electronic Structures of Ag-adsorbed Si NC-AFM Tips", Applied Surface Science Vol.188, pp.331-334, 2002.5

邦文題目：非接触AFMのAg吸着Si探針の原子・電子構造に関する理論的研究

We have studied the atomic and electronic structures of Ag-adsorbed Si NC-AFM tips using cluster models and ab initio calculations within the local spin density functional approach as the first step to clarify the tip effects on NC-AFM

images. On the contrary to simple guess that the most stable position for a Ag adsorbate is just below the apex Si atom, the most favorable position was found where the Ag adsorbate bonds to both the apex and one of the second-layer Si atoms. In these two positions, the distributions of the highest occupied molecular orbitals are distinctly different from each other. Further, we have fouhd that the energy barrier for transition between the two positions is only a few tenths of eV. This suggests that the Ag adsorbate may drift within a wide area around the tip apex at room temperature.

S. Furuya, Y. Gohda, N. Sasaki and S. Watanabe : "Ab Initio Calculation of the Electric Properties of Al Atomic Chains under Finite Bias Voltages", Japanese Journal of Applied Physics, Vol.41, pp.L989-L991, 2002.9

邦文題目：有限バイアス電圧下でのAl原子鎖電子状態の非経験的計算

We have analyzed electric conduction through Al atomic chains between two jellium electrodes by ab intio calculations focusing on their dependences on bias voltages (V_bias > 3V) as the number of atoms increases, whereas the current is roughly independent of the number of atoms at low bias voltages. This result can be understood if we assume that resonant conduction through states spreading over the entire chains is destroyed in the cases of Al4 and Al5 at high bias voltages.

Y. Izumi, S. Okamoto, K. Takizawa and K. Tanaka : "Improving the Light Out-Coupling Properties of Inorganic Thin-Film Electroluminescent Devices", Jpn. J. Appl. Phys. Vol.41, Part 1, No.3A, pp.1284-1287, 2002

邦文題目：無機薄膜ELデバイスの光出力特性の改善

The light out-coupling properties of inorganic thin-film electroluminescent devices can be improved by using a new device structure with a light-scattering layer. This consists of particles dispersed in a binder and it can be laminated on the surface of conventional devices by screen-printing. The light-scattering layer increases the luminance to approximately three times that of conventional devices and reduces the viewing-angle dependence of the electroluminescent spectrum.

T. Fujii, H. Fujikake, K. Takizawa, T. Hirabayashi, Y. Tanaka, K. Hirakata, H. Asakawa, T. Tamura, H. Kita, K. Hara and K. Tanaka : "Light-Controllable Spot Luminaires Using a Liquid Crystal Light Shutter and a High-Intensity Discharge Lamp", J. Light & Vis. Env., Vol.26, No.1, pp.13-23, 2002

邦文題目：液晶シャッタと高輝度放電灯を用いた調光機能付照明装置

New types of light-controllable luminaires using a metal halide lamp or a xenon lamp with a liquid crystal light shutter have been developed and demonstrated for spot or beam spot lighting of television program production. We fabricated a novel liquid crystal light shutter using a heat-resistant composite film of polymer and liquid crystal materials with a wide range of operating temperatures up to 150C. The light shutter can modulate a strong luminous flux from the high-intensity discharge lamps, instead of a conventional mechanical shutter which has problems such as generating acoustic noise and being slow and heavy. The light modulation of the light shutter is based on a light scattering effect and the degree of scattering is controlled by the voltage applied to the shutter. It exhibits attractive features such as high transmittance, high-speed response, and high extinction ratio. The luminous intensity of an object could be varied continuously using the luminaires with the shutter, and the chromaticity deviation was drastically decreased by driving it with pulse width modulation.

H. Fujikake, T. Murashige, J. Yonai, H. Kikuchi, M. Kawakita and K. Takizawa : "Electrooptical Properties Free-Standing Polymer-Stabilized Ferroelectric Liquid Crystal Films", Electronics and Communication in Japan, Part 2, Vol.85, No.5, pp.35-42, 2002

邦文題目：高分子安定化強誘電性液晶の電気光学特性

We evaluated the electrooptical properties of free-standing films based on ferroelectric liquid crystals stabilized by a rigid aligned polymer

network in anticipation of future development of lightweight, large-area flexible film displays. It was shown that the mechanical strength of the film increased at higher concentration of added monomer, while the speed of electrooptical response declined. This could be a result of restricted switching of the liquid crystal molecules due to their interaction with the surface of the solidified polymer. Although the contrast ratio decreased at higher polymer concentrations, when the concentration of the dispersed polymer was high enough to provide free-standing ability, 100:1 or higher contrast ratios were achieved. In addition, the threshold voltage required for liquid crystal molecular switching was spatially changed due to polymer dispersion, resulting in the appearance of a grayscale display function.

M. Tomiya and N. Yoshinaga : "Numerical Analysis of Level Statistical Properties of Two- and Three-Dimensional Coupled Quartic Oscillators", Computational Physics Communications, Vol.142, No.1-3, pp.82-87, 2001.12

The spectral statistical properties, i.e. the nearest neighbor spacing distribution, the spectral rigidity and the mode fluctuation distribution (MFD) are numerically studied for two- and three-dimensional quantum coupled oscillators. By changing a single parameter, the system is continuously transformed from an integrable system to a chaotic one. The diagonalization method of the truncated Hamiltonian matrix is shown to be effective for the calculation of quantum spectra. The MFD is found to be more sensitive to the intebrability of the system than its chaoticity. The Poincaré surface of three-dimensional systems are discussed.

M. Tomiya and N. Yoshinaga : "New Approach to Level Statistics of Coupled Quartic Oscillators", Computational Physics Communications, Vol.142, No.1-3, pp.88-94, 2001.12

The nearest neighbor level spacing distribution (MFD) for two-dimensional coupled quartic oscillators is studied numerically. The NNSD of the systems is fitted to the Berry-Robnik (BR) distribution, the Brody distribution and the Berry-Robnik-Brody (BRB) distribution which was proposed by M. Robnik and recently applied to the spectrum of nuclei by V. Lopac. The BRB distribution is found to be the most properly fitted to the NNSD for the whole range from the integrable limit to the chaotic regime. The new interpolation formula between the Poisson and the Wigner distribution is proposed.

M. Tomiya and S. Kikuchi : "Application of Modified Counter-Propagation for Satellite Image Classification", International Archives of Photogrammetry and Remote Sensing, Vol.34, Part 3B, Commission 3, pp.277-282, 2002.9

A supervised category classifier for satellite images by using the Modified Counter-Propagation (MCP) is proposed. The MCP is a neural network which consists of three layers: the input layer, the competition layer and the output layer. The input and the competition layers form the Self-Organizing Map (SOM). The connections of Counter-Propagation from the competition layer are extended to the output layer. The Landsat image data are adopted as the input data of the MCP, and the output layer consists of the pixel values, which represent categories to be classified. Our result shows that the MCP can classify more accurate and precise than that of the SOM only, especially for the classification of vegetation, farm and wood.

大川賢治・中野武雄・馬場　茂：「スパッタCu膜の表面ラフネス成長のスケーリング観察」真空，45巻，3号，pp.134-137, 2002.3

Scaling analysis of surface roughness has been performed on copper films prepared by DC magnetron sputter deposition. The deposition was performed in argon pressures of 2 and 10 Pa. In both pressures, deposition rates were almost same at 1.1 nm/s. Self-affine parameters α and β were determined from a series of AFM topographs of films with various deposition times (30~180 min). At 10 Pa, roughness parameter α was 0.6~0.7 and the dynamical parameter β was 0.9, while at 2 Pa, where the surface rough-

ness grew more modestly, α was 0.5~0.7 and β was 0.6. The difference in both pressures also appeared in correlation length ξ. As the general roughness growth model predicted, it became larger as deposition proceeded at 10 Pa. On the other hand, it stayed almost constant at 2 Pa. Possible reasons are discussed from the viewpoint of roughness growth mechanism.

中野武雄:「中高圧力下 (2～20 Pa) のスパッタリングにおける粒子輸送過程」真空, 45巻, 9号, pp.699-705, 2002.9

Transport process of sputtered atoms becomes more complex in mid-to-high pressure environment (2~20 Pa). At high pressures, sputtered atoms collide with ambient gas atoms frequently, and are ready to thermalize. We have been studying the situation with both Monte-Carlo (MC) computer simulation and experiment. We have extended the MC simulation in two ways: One is the formulation of the relative motion of the colliding gas atom against the sputtered atom, and the other is the description of the flow of decelerated atoms with a diffusion equation. This new simulation has been applied to the pressure dependence of the thickness profile of sputtered Cu films, and also to that of the film composition in the case of the sputter deposition from LaB_6 target. It has been found experimentally that the relative Cu deposition ratio on hidden faces takes the maximum and the B/La ratio takes the minimum, both at midst pressure. Numerical simulation agrees well with the experimental results, and we conclude that these experimental behaviour can be ascribed to the thermalization of sputtered particles.

一　般　教　養

K. Tanaka, Y. Yamamoto, H. Obara, and S. Iwata : "Quinone-Recognition by Four-Point Hydrogen Bonding in Porphyrin System Having Urea Moiety" Supramolecular Chemistry, 14 (4), pp.347-352, 2002.7

邦文題目：ウレア置換基をもつポルフィリンの4点水素結合によるキノン認識

5,15-cis-Bis(ureidophenyl)porphyrins have significant recognizing ability for *p*-benzoquinones through four-point hydrogen bonding. Although an unusual temperature-dependence of the complexation is observed with bis(*N'*-phenylureidophenyl) porphyrin, bis(*N'*-ethylureidophenyl)porphyrin shows a satisfactorily linear van't Hoff plot and recognizes an electron-rich *p*-benzoquinone such as tetramethyl-*p*-benzoquinone more effectively, which is ascribed to the large enthalpy change in the complex.

I. Wakabayashi : "Families of Cubic Thue Equations", Analytic Number Theory / eds. C. Jia and K. Matsumoto, Developments in Mathematics, Kluwer, Vol.6, pp.359-377, 2002

邦文題名：３次トゥーエ方程式について

We survey results on families of cubic Thue equations. We also state new results on the family of cubic Thue inequalities $|x^3+axy^2+by^3| \leqq k$, where a,k are positive integers and b is an integer. We give upper bounds for the solutions of these inequalities when a is larger than a certain value depending on b, and as an example, for the case b=1,2, $a \geqq 1$, and $k=a+b+1$, we solve these inequalities completely. Our method is based on Padé approximations.